Hydrophobic Substitutions in the First Residue of the CRAC Segment of the gp41 Protein of HIV†

Sundaram A. Vishwanathan,‡ Annick Thomas,§ Robert Brasseur,§ Raquel F. Epand,|| Eric Hunter,‡ and Richard M. Epand*,||

Emory Vaccine Research Center, Yerkes, Emory University, 954 Gatewood Rd, Atlanta, Georgia 30329, Department of Biochemistry and Biomedical Sciences, McMaster University, 1200 Main Street West, Hamilton, Ontario L8N 3Z5, Canada, and Faculté Universitaire des Sciences Agronomiques de Gembloux Centre de Biophysique Moléculaire Numérique, Passage des Déportés, 2 5030 Gembloux, Belgium

Received September 14, 2007; Revised Manuscript Received October 24, 2007

ABSTRACT: We investigated the peptides *N*-acetyl-AWYIK-amide and *N*-acetyl-VWYIK-amide corresponding to single amino acid substitutions in LWYIK, a segment found in the gp41 protein of HIV and believed to play a role in sequestering this protein to a cholesterol-rich domain in the membrane. The effects of these peptides on the thermotropic phase transitions of 1-stearoyl-2-oleoylphosphatidylcholine (SOPC) and mixtures of SOPC and cholesterol were intermediate between that having the wild-type sequence (LWYIK) and another (IWYIK), the least active peptide previously studied. This correlated with results from studies of single mutations in the gp41 protein of HIV-1, in which L^{679} of the LWYIK segment is replaced with either A or V, measuring the capability of TZM-BL HeLa-based HIV-1 indicator cells to form syncytia. The peptides were also comparatively analyzed in silico. All together, the results suggest that the mode of interaction of this region of gp41 with the polar heads of membrane lipids contributes to its cholesterol selectivity and that this is somehow related to the biological activity of the viral glycoprotein.

The ectodomain adjacent to the single transmembrane helix of the gp41 protein of HIV[1] has the sequence KWASLWNWFNITNWLWYIK and is referred to as the Trp-rich juxtamembrane segment. Mutations in this region reduce infectivity, indicating a role in viral entry (*1*). It has recently been suggested that the fusion peptide-proximal polar segment and the Trp-rich juxtamembrane segment interact during the fusion process (*2*). The carboxyl terminus of this juxtamembrane region is LWYIK. This segment is highly conserved among HIV-1 strains. LWYIK has been shown in other contexts to play a role in cholesterol recognition. Linking LWYIK to the maltose binding protein endows it with the property to bind to cholesterol-hemisuccinate agarose (*3*). In addition, we showed that the peptide *N*-acetyl-LWYIK-amide caused the redistribution of cholesterol into domains and that cholesterol facilitated the insertion of the peptide into a membrane (*4*). The segment LWYIK is called a CRAC motif, and it is found in several proteins that interact with cholesterol. A CRAC motif is defined as a sequence pattern -L/V-$(X)_{(1-5)}$-Y-$(X)_{(1-5)}$-R/K-, in which $(-X-)_{(1-5)}$ represents between one to five residues of any amino acid (*5*). The loose requirements for a CRAC domain predicts that a large number of sequences would favor interaction with cholesterol (*6*). We have begun to test the accuracy of the CRAC motif for predicting cholesterol binding by studying several different peptides made by replacing individual residues of *N*-acetyl-LWYIK-amide (*7*). Among the seven mutations we tested, the natural sequence was the most potent in sequestering cholesterol, while surprisingly the least potent was *N*-acetyl-IWYIK-amide that differs only by the movement of one CH_3 group, i.e., they are structural isomers. In addition, membrane fusion studies in cells, comparing the intact gp41 and the L679I mutant, demonstrated that the single conservative mutation in this CRAC domain caused a marked decrease in the fusion of TZM-BL HeLa cells (*7*). In the present work, we extend these studies by substituting either Val or Ala for Leu in both the peptide *N*-acetyl-LWYIK-amide for studies of cholesterol interactions, as well as at position 679 in the intact gp41 protein to assess the consequences on membrane fusion in a biological setting. VWYIK is a peptide with similar hydrophobicity as LWYIK and one that also corresponds to a CRAC segment

† This work was supported by the Canadian Institutes of Health Research (grant MOP-85008) and the "Ministère de la Région Wallonne" contract no. 14540 (PROTMEM). We would also like to thank the "FRSM" (contract n°3.4505.02) for financial support. The work on mutagenesis and HIV-1 fusion was supported by grant R01 AI-33319 from the National Institutes of Health. R.B. is Research Director at the National Funds for Scientific Research of Belgium (FNRS). A.T. is Research Director at the "Institut National de la Santé et de la Recherche Médicale" (INSERM France). R.M.E. is a Senior Research Investigator of the Canadian Institutes for Health Research.

* Corresponding author. Tel: 905-525-9140, ext. 22073. Fax: 905-521-1397. E-mail: epand@mcmaster.ca.

‡ Emory University.

|| McMaster University.

§ Faculté Universitaire des Sciences Agronomiques de Gembloux Centre de Biophysique Moléculaire Numérique.

[1] Abbreviations : CRAC, cholesterol recognition/interaction amino acid consensus; HIV, human immunodeficiency virus; PC, phosphatidylcholine; SOPC, 1-stearoyl-2-oleoylphosphatidylcholine; DSC, differential scanning calorimetry; T_m, phase transition temperature; ΔH, calorimetric enthalpy; MPER, the membrane-proximal external region; MFP, mean force potential.

10.1021/bi7018892 CCC: $40.75
Published on Web 12/15/2007

but is not present among the sequences of gp41 of known strains of HIV. In contrast, AWYIK does not comply with the rules for a CRAC motif and is less hydrophobic. VWYIK is also slightly less hydrophobic than the wild-type LWYIK, having one less CH_2 group, and it is also more conformationally restricted, having two methyl substitutions on the β-carbon. The present studies will address the question of whether L is the only residue that can be accommodated in this position without significant loss of function, either with regard to cholesterol sequestration or fusogenicity.

MATERIALS AND METHODS

Materials. The peptides are all *N*-acetyl-peptide-amides, i.e., blocked at the terminal amino and carboxyl groups. The peptides were synthesized by Synbiosci Corp. (Livermore, CA) and purified by HPLC to >95% purity. Phospholipids and cholesterol were purchased from Avanti Polar Lipids (Alabaster, AL).

Preparation of Samples for DSC. Phospholipid and cholesterol were codissolved in chloroform/methanol (2/1, v/v). For samples containing peptide, an aliquot of a solution of the peptide in methanol was added to the lipid solution in chloroform/methanol. The solvent was then evaporated under a stream of nitrogen with constant rotation of a test tube so as to deposit a uniform film of lipid over the bottom third of the tube. The last traces of solvent were removed by placing the tube under high vacuum for at least 3 h. The lipid film was then hydrated with 20 mM PIPES, 1 mM EDTA, 150 mM NaCl with 0.002% NaN_3 (pH 7.40) and suspended by intermittent vortexing and heating to 50 °C over a period of 2 min under argon.

Differential Scanning Calorimetry (DSC). Measurements were made using a Nano differential scanning calorimeter (Calorimetry Sciences Corp., Lindon, UT). The scan rate was 2 °C/min and there was a delay of 5 min between sequential scans in a series to allow for thermal equilibration. The features of the design of this instrument have been described (*8*). DSC curves were analyzed by using the fitting program DA-2, provided by Microcal Inc. (Northampton, MA), and plotted with Origin, version 5.0.

Modeling. (i) Structure Properties. A search was made for the most favorable conformation of each of the peptides by using PepLook (*9*). The energy of peptide conformations is calculated by an all atom description of structures with the addition of van der Waals, electrostatic, and internal and external hydrophobicity energy terms. The van der Waals contribution was calculated using the 6-12 Lennard-Jones description of the energy of interactions between unbonded atoms (*10*). The Coulomb's equation was used for electrostatic interactions between unbonded charged atoms with a dielectric "constant" sigmoidally varying from 1 to 80 for the region between atoms and using FCPAC partial atomic charges (*11*). The intramolecular hydrophobicity contribution to stability was calculated using atomic Etr (energy of transfer) and the fractions of atomic surface covered by the atoms in interactions. Seven atomic types are used for calculating Etr (*12*). When structures are calculated in water, the contribution of solvent is accounted for by an external hydrophobicity energy term where the solvent-accessible surface of atoms is calculated by the method of Shrake and Rupley with 162 points (*13*−*15*). From the 500 000 calculated structures, the 100 most stable are sorted, compared by structure fitting and clustered by rms deviation less than 1 Å. Each cluster is represented by its lowest energy model. Calculations are run in water, in lipids, and at a membrane interface. All cluster models are tested for membrane insertion.

(ii) Membrane Insertion. Insertion into the membrane was tested with the IMPALA systematic program (*16*). The minimal restraint energy profile of insertion of each peptide into the membrane was determined by inserting separately the previously selected structures in the membrane. Each molecule was moved every 1 Å step across the bilayer (*z* axis) and was rotated in the *zx* plane (5000 positions over 360°) at each step. The insertion profile of one peptide in the membrane was set as the combination of the minima at all steps; hence, the profile could account for a different structure and a different angle of insertion at each level of the membrane.

(iii) Cholesterol−*Peptide Interactions.* Determining the interactions of the most stable conformation of each peptide in a membrane with cholesterol extended the analysis. The best IMPALA position was used for each peptide conformation and the best position for the cholesterol in the membrane. The two molecules were tested in the calculation varying the position of cholesterol in the vertical (*z*-axis) and horizontal (around the CRAC peptide) directions as well as by self-rotation around the long axis of cholesterol. All together 5 720 400 relative positions between each peptide conformation and sterol were tested to finally retain the conformation of maximal intermolecular interactions. The best complex among all complexes formed was evaluated on the basis of it having optimal (i.e., minimal) values of intra- and intermolecule energies.

Cell−*Cell Fusion. (i) Cell Culture*. 293T and TZM-BL cells were used for fusion assays. TZM-BL HeLa-based HIV-1 indicator cells (*17*) that show a high susceptibility to HIV-1 infection were kindly provided by Tranzyme Inc., Birmingham, AL. These cells contain reporter genes, luciferase, and β-galactosidase, that are expressed in the presence of Tat, under the influence of HIV-1 LTR. Cells were subcultured every 3−4 days by trypsinization and maintained in Dulbecco's modified Eagle medium (DMEM) supplemented with 10% fetal bovine serum and antibiotics.

(ii) Mutagenesis and Plasmid Vectors. An NL4.3 (laboratory-adapted X4 strain) *Kpn*I−*Bam*HI envelope fragment was cloned into vector pSP72. Mutations L679A and L679V of the HIV-1 membrane-proximal external region (MPER) were designed using QuikChange (Stratagene, La Jolla, CA). The mutated envelope gene fragment was subsequently polymerase chain reaction amplified and cloned into pCDNA3.1/V5-His-TOPO as per the manufacturer's instructions (Invitrogen, Carlsbad, CA).

(iii) Cell−*Ccell Fusion Assays.* 293T cells were transfected with pCDNA constructs expressing wild-type and mutant HIV-1 envelopes using Fugene 6 transfection reagent (Roche Diagnostics Corp., Indianapolis, IN). Twenty hours post-transfection, they were mixed in a 1:5 ratio with TZM-BL cells and replated in 24-well plates. After 20 h, the cells were microscopically examined for fusion by counting the blue syncytia and the number of nuclei/syncytium following addition of 5-bromo-4-chloro-3-indolyl-β-D-galactopyranoside (X-gal; Promega, Madison, WI) as described by

Table 1: Effect of Various Peptides[a] on Enthalpies of the Chain Melting Transition of SOPC (cal/mol SOPC)

mol % peptide	LWYIK[b]	IWYIK[b]	VWYIK	AWYIK
0		3800		
5	3800	3600	2500	3500
10	3800	3200	2000	2500
15	3800	2600	2000	2400

[a] Peptides are *N*-acetyl-peptide-amides. [b] Data taken from ref *7*.

Table 2: Effect of Various Peptides[a] on Enthalpies of the Chain Melting Transition of SOPC/Cholesterol (7/3) (cal/mol SOPC)

mol % peptide	LWYIK[b]	IWYIK[b]	VWYIK	AWYIK
0		520		
5	1000	~0	70	150
10	1100	~0	200	250
15	1200	~0	60	150

[a] Peptides are *N*-acetyl-peptide-amides. [b] Data taken from ref *7*.

Kimpton and Emerman (*18*). Fusion was also evaluated by measuring luciferase activity (Luciferase Assay System, Promega) according to the manufacturer's protocol. All fusion assays were done in triplicate.

(iv) Cell Surface Expression of Env Proteins. The pCDNA3.1 vectors encoding WT and mutant Envs were transfected into 293T cells in six-well plates. At 36−40 h posttransfection, the cells were trypsinized and washed in flow cytometry buffer (PBS with 0.1% BSA and 0.1% NaN_3). Cells were resuspended in 500 μL of buffer. Cell-surface-associated Env molecules were fluorescently labeled by incubating 100 μL of harvested 293T cells with 0.5 μg/mL of gp120-specific b12 (a gift from Dr. Dennis Burton, Scripps Research Institute, La Jolla, CA) at room temperature for 1 h. This antibody had been labeled with Alexa Fluor647 (Invitrogen) according to the manufacturer's instructions. The Env staining was evaluated by flow cytometry with FACSCalibur (Becton Dickinson, Franklin Lakes, NJ); the data were analyzed using FloJo software version 8.2 (Tree Star Inc., Ashland, OR), and the mean fluorescence intensity (MFI) was calculated from the acquisition of at least 30 000 gated events. Nonspecific background fluorescence due to the secondary antibody was subtracted from the MFIs.

RESULTS

DSC. DSC can be used to assess the effect of peptides on the miscibility of cholesterol and SOPC (*19*). In the presence of cholesterol, the melting transition of SOPC is broader and has a reduced transition enthalpy. If a peptide promotes the rearrangement of cholesterol into cholesterol-rich domains, the remaining SOPC-rich domains will exhibit a more cooperative (sharper) phase transition of higher enthalpy. With SOPC, this is most easily discerned in the cooling scans because of the low transition temperature of this phospholipid. The phase behavior of SOPC with several mole fractions of cholesterol in the presence of different mole fractions of *N*-acetyl-LWYIK-amide (*4*) or *N*-acetyl-IWYIK-amide (*7*) has been presented. In this work, we compare the effects of *N*-acetyl-AWYIK-amide and *N*-acetyl-VWYIK-amide with those of *N*-acetyl-LWYIK-amide and *N*-acetyl-IWYIK-amide on the enthalpies of SOPC (Table 1) or with SOPC/cholesterol (7/3) (Table 2).

Another consequence of the formation of cholesterol-rich domains can be that the sterol passes its solubility limit in a region of the membrane, forming crystallites. Anhydrous crystalline cholesterol is known to undergo a crystalline polymorphic phase transition at 38 °C on heating and at 23 °C on cooling at a scan rate of 2°/min (*20*), with an enthalpy of 910 cal/mol (*21*). This hysteresis is characteristic of anhydrous cholesterol crystals and provides a criterion for identifying its presence. At a SOPC/cholesterol molar ratio of 7/3, no cholesterol crystals, or at most traces of crystalline cholesterol, are found with the lipid alone or in the presence of up to 15 mol % of any of the peptides. However, at a SOPC/cholesterol molar ratio of 6/4, anhydrous cholesterol crystals can be detected with *N*-acetyl-AWYIK-amide as well as *N*-acetyl-LWYIK-amide. At a 1:1 mixture of SOPC and cholesterol there is still no deposition of cholesterol in the absence of peptide, but with this lipid mixture, none or only a trace of crystalline cholesterol is found with *N*-acetyl-AWYIK-amide or with *N*-acetyl-VWYIK-amide. This behavior is different from that of *N*-acetyl-LWYIK-amide, which does cause the deposition of cholesterol crystals with this lipid mixture (*4*). There are two mechanisms by which peptides can promote the formation of cholesterol-rich domains: one is by preferentially binding to these domains and stabilizing them and the other is by being excluded from these domains and preferentially binding to cholesterol-depleted regions of the membrane, forcing cholesterol into another region of the membrane (*22*). From the formation of cholesterol crystallites it is not possible to distinguish between these two possibilities. In the case of peptides that sequester into cholesterol-rich domains, they will only cause the formation of cholesterol crystallites from the fraction of cholesterol that the peptide is not directly bound to. Cholesterol that is bound to peptide has a lower probability of forming crystals. In the case of *N*-acetyl-AWYIK-amide, the amount of cholesterol crystals formed does not increase proportionally to peptide concentration. Thus, although there is some formation of cholesterol crystals with *N*-acetyl-AWYIK-amide and *N*-acetyl-VWYIK-amide, as indicated by the characteristic different temperatures of the transition on heating and cooling, it is much less than that previously found with *N*-acetyl-LWYIK-amide (*4*).

Modeling. 3D structures of the four peptides were calculated in conditions of hydrophilic, interfacial, and hydrophobic media. Their intrinsic stability were analyzed on the basis of mean force potential (MFP) and electrostatic potential of all models in the different medium (Figures 1 and 2). The mean MFP values of the LWYIK models at the interface are the largest, supporting the conclusion that this peptide has the best possibilities of intrinsic stability especially in a membrane interface (Figure 1). The models of IWYIK, AWYIK, and VWYIK elicit higher MFP values and no clear difference in the different media. MFP values are poorly representative of electrostatic interactions, because in peptides, as in proteins, interactions between charged atoms are less frequent than interactions between apolar atoms. Hence, we specifically examined intramolecular electrostatic interactions. Differences in electrostatic intramolecular interactions can only be due to differences in peptide conformations, since the sequences differ by a noncharged side chain. Here again, LWYIK at the interface has the best

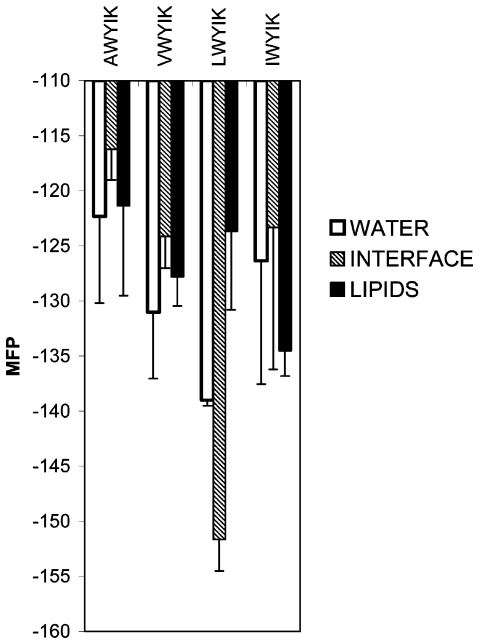

FIGURE 1: Mean force potential values of all calculated 3D models of AWYIK, VWYIK, LWYIK, and IWYIK (mean ± SD of 99 models). Models were calculated using the Boltzmann stochastic procedure of PepLook (*9*) in hydrophilic (water), hydrophobic (lipids), and interfacial conditions. MFP values of peptides (kcal) were calculated by summing the MFP values of each amino acid. The latter was calculated using MFP functions describing atom−atom interactions with a cutoff distance of 10 Å (*9*).

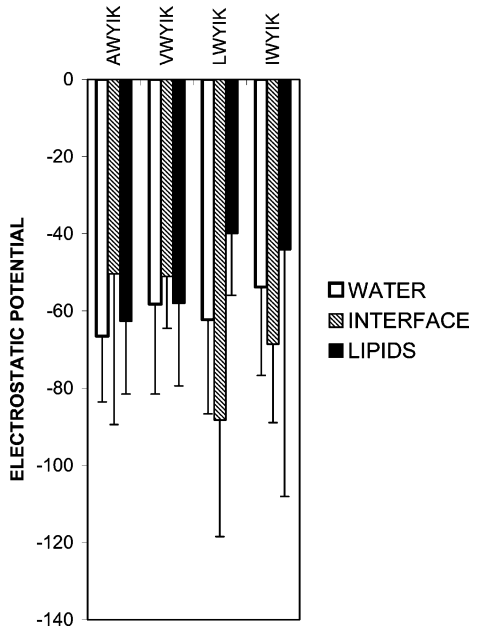

FIGURE 2: Intramolecular electrostatic interactions of the 3D models of AWYIK, VWYIK, LWYIK, and IWYIK calculated using PepLook (mean ± SD). Models were calculated as described in Figure 1. The electrostatic energy of interaction (kcal) were calculated by summing the contribution calculated for each atom. Atom contribution was calculated using a Coulomb energy function, the FCPAC partial atomic charges (*26*), and a sigmoidal variation of the dielectric constant with interatomic distance.

intrinsic stability in electrostatic interactions, although the differences are less marked because fluctuations between the different models of a peptide are larger than fluctuations of MFP (Figure 2 compared to Figure 1).

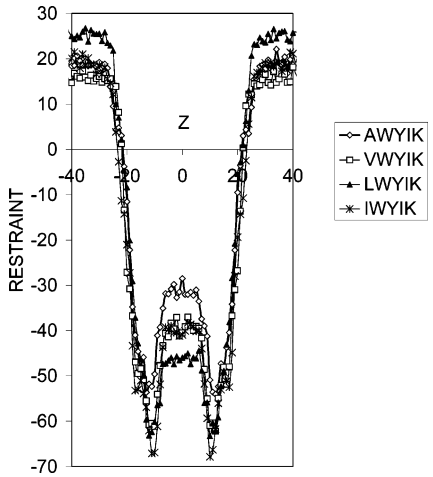

FIGURE 3: Restraint value of peptide traversing across a membrane; In this plot, the *z*-axis is perpendicular to the membrane surface (angstroms), zero being the membrane center and 18.5 Å the membrane/water interface. The systematic procedure of IMPALA is run as described in Methods and Materials. The plot shows the envelop of minimal restraint energy (kcal/mol) that combines the results obtained with all models of structures obtained with PepLook. The *z* value maps the peptide mass center.

All models were tested in a membrane by a systematic procedure that forces the molecule across the bilayer and calculates the restraint energy envelope. The restraint envelope of a peptide was derived from the insertion of all models by assuming that a peptide can shift from one conformation to another at any membrane level to fit the external medium optimally. Using reference Etr values of amino acids calculated from atomic Etr (*23*), the elongated common WYIK sequence fragment has a slightly positive transfer energy (+3.96 kcal/mol) and hence is slightly hydrophilic. Adding a hydrophobic N-end and folding the structure to bury one or the other chemical moiety will determine differences in solubility.

The differences in restraint profiles of the peptides are small (Figure 3). All models of peptides prefer being at the interface rather than in water or in the lipid core. The most stable at the interface is IWYIK, the difference with LWYIK being small. Next we analyzed the cholesterol−peptide interaction: all peptides generated electrostatic interactions with the OH polar head of cholesterol, at least as a H-donor or as a H-acceptor, but none was simultaneously a H-acceptor and donor as previously found for LWYIK. This is not due to the location of polar atoms because all peptides locate several of their backbone atoms in the interface. It is obvious that the 3D folding of the peptides' fragment is crucial to regulate the apparent hydrophobicity, and changing the N-end changes both the hydrophobicity and the folding plasticity.

Mutagenesis of the Membrane-Proximal External Region (MPER) of HIV-1 gp41. We examined the effects of mutations in the LWYIK segment in the context of the entire HIV-1 Env. This peptide is part of the HIV-1 MPER in the gp41 ectodomain whose crucial role in viral fusion has been established (*1*). We employed the QuikChange mutagenesis method to substitute leucine (L) at position 679 with either alanine (A) or valine (V). The mutation was introduced in the *Kpn*I−*Bam*HI NL4.3 envelope fragment that had been subcloned into vector pSP72. The mutated envelope fragment was then subcloned into the envelope expression vector

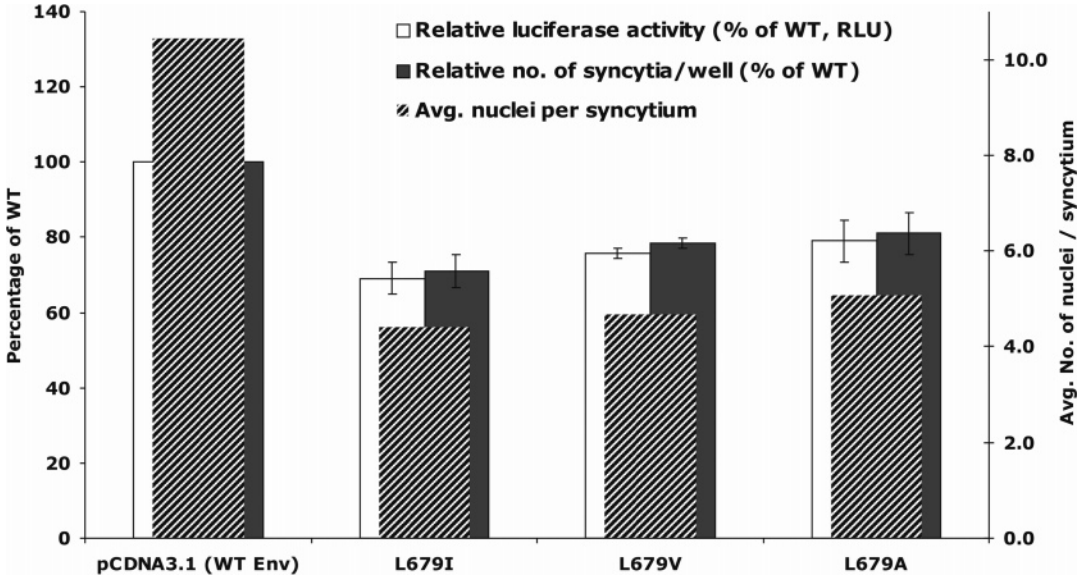

FIGURE 4: Cell−cell fusion assays of wild-type and MPER mutants L679V, L679A, and L679I. Data shown are the average of three experiments, for each of which samples were run in duplicate. The number of syncytia per well was determined by counting the syncytia in each well (24-well plate) and averaging the total for each mutant. The number of nuclei per syncytium was determined by counting the nuclei in 20 syncytia per well. Luciferase activity (RLU, relative light units) was determined as per the manufacturer's instructions and normalized as a percentage of that observed with the wild-type.

pCDNA3.1/V5-His-TOPO. All mutations were confirmed by sequencing.

Effects on Cell−Cell Fusion. The fusion efficiency of all three mutations of L679 was between 69 and 79% that of the wild-type protein, as assessed by the luciferase assay (Figure 4). The L679I mutant showed the least fusion, while the L679A and L679V showed similar patterns (A being slightly higher than V). The β-galactosidase assay gave similar results (Figure 4, number of syncytia per well). The average number of nuclei per syncytium is lowest for I and highest for A (Figure 4).

Cell Surface Expression of Env Proteins. In our earlier study of the L679I mutation, we did not assess the level of surface expression of the protein in the transfected cells (*7*). In the present study, we show that there is only a small reduction in cell surface expression of any of the mutants, relative to the wild-type protein taken as 100%. Expression levels for the mutant (as % of wild type) were 79 ± 13 for L679A, 77 ± 12 for L679V, and 73 ± 11 for L679I.

DISCUSSION

Among the sequences LWYIK, IWYIK, VWYIK, and AWYIK, the one that exhibits the greatest selectivity for cholesterol over phosphatidylcholine is the wild-type sequence, LWYIK. The *N*-acetyl-LWYIK-amide is the only one that does not lower the enthalpy of pure SOPC, even at 15 mol % peptide (Table 1). In addition, *N*-acetyl-LWYIK-amide is the only peptide that, in mixtures of SOPC and cholesterol at a 7:3 molar ratio, causes the enthalpy of the SOPC transition to increase (Table 2). Thus, LWYIK exhibits preferential interaction with cholesterol-rich domains, resulting in a clearing of part of the membrane from cholesterol.

The VWYIK and AWYIK peptides have behavior that is intermediate between those of LWYIK and IWYIK with mixtures of SOPC and cholesterol (Table 2). VWYIK and AWYIK preferentially locate at the membrane interface and both induce only partial loss of the SOPC transition enthalpy in SOPC/cholesterol 7/3. IWYIK and LWYIK also preferentially locate at the interface, but IWYIK eliminates this transition completely, in contrast with LWYIK, which enhances the transition enthalpy (Table 2). A decrease in the transition enthalpy would not be caused by the redistribution of cholesterol but rather more likely by the peptide interacting with both lipid components and broadening the transition. This effect is stronger for IWYIK than for either VWYIK or AWYIK. Interestingly, we noticed that IWYIK has the largest diversity in structure diversity at the interface. Indeed, we previously reported that IWYIK has less structural diversity in the hydrophobic medium, and this is true in the present calculations, too. However, surprisingly and unlike the other peptides, IWYIK shows five different structures at the interface, whereas there are only two for LWYIK and three for AWYIK and VWYIK (Figure 5).

Thus, connecting experimental and modeling data might make sense if one considers that the structural diversity of IWYIK opens it to the capacity to bind either PC or cholesterol polar heads, whereas LWYIK has an optimal binding cavity for the polar head of cholesterol with a well-positioned H-donor and H-acceptor. Hence, LWYIK selectivity would be linked to a more fitted interaction for cholesterol, whereas the other peptides will interact either as H-donor or as H-acceptor with cholesterol and as H-donor with the phosphatidylcholine polar head.

This group of four peptides has an interesting relationship to the algorithm predicting "CRAC sequences" that interact with cholesterol-rich domains (*5*). The wild-type sequence, LWYIK, was identified as a cholesterol-interacting segment because it fulfilled the requirements of a CRAC domain (*4*). However, VWYIK also corresponds to a CRAC segment, yet it is much less potent than LWYIK in preferentially interacting with cholesterol and is similar in this regard to AWYIK, which is not a CRAC sequence. Hence, the CRAC algorithm simply restricted to a sequence motif is useful for suggesting potential protein segments but lacks the 3D

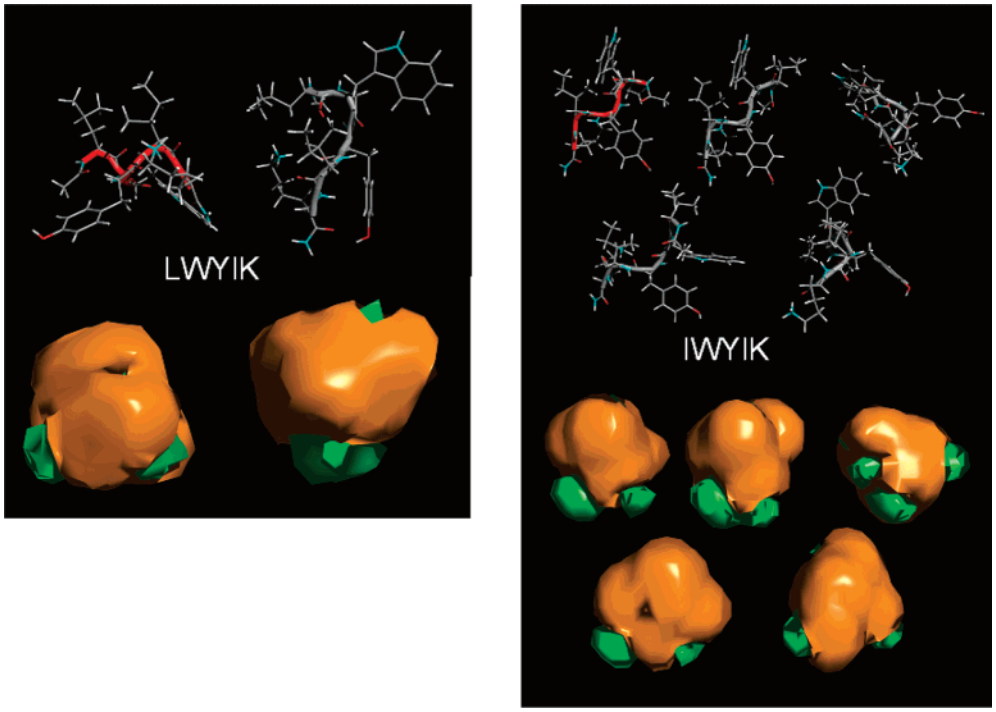

FIGURE 5: LWYIK and IWYIK PepLook models of 3D structures at the interface. As explained in methods, the 99 structures selected with PepLook were clustered into subpopulations on the basis of a structure fitting and rms deviation > 1.0 Å. Each cluster is represented by its model of lower intramolecular and membrane restraint energies. On the left, the two models of LWYIK clusters, on the right, the five models of IWYIK clusters. Models are shown according to their position at the interface (up is hydrophobic, down is hydrophilic). (Top) The atomic structures; the backbone is fitted by a tube (red for the Prime structure, gray for the others). (Bottom) The MHP surfaces (molecular hydrophobicity potential); the hydrophilic isopotential surface of 0.1 kcal/mol is green, and the hydrophobic isopotential surface of −0.1 kcal/mol is brown. MHP surfaces are calculated by taking into account the contribution of all atoms as previously described (*23*).

elements important for specific sequences. Cholesterol selectivity may require the capacity of the segment to form a three-dimensional cavity for the cholesterol polar head.

There is very good phenomenological correlation between the behavior of these protein segments with model membranes with regard to interaction with cholesterol and the fusogenic potency of mutant forms of the gp41 protein of HIV expressed in cells. One would not expect an exact agreement, as other factors in addition to cholesterol interactions undoubtedly affect fusogenic activity. We have previously shown that the L679I mutant of gp41, containing the protein segment IWYIK, had significantly less fusogenic activity compared with the wild type protein (*7*). Two newly constructed mutant forms of gp41 were expressed, L679V and L679A. These new constructs also showed reduced fusogenicity, but the loss of activity was somewhat less than for L679I (Figure 4). A previous report, qualitatively showing reduced fusogenicity of the L679A mutant, agrees with the present result (*24*). The difference in cell surface expression among the mutants is small and within experimental error. However, the mutants have a slightly lower level of expression than the wild-type protein. This could make a small contribution to, but not fully account for, the weaker fusogenic activity of the mutants compared with the wild-type gp41. Previous studies from the Hunter laboratory demonstrated that, in order to obtain a 50% decrease in fusion from the Env of SIV, a 10-fold difference in expression level was required (*25*). In the present study, a decrease of approximately 20% in the expression level leads to almost a 50% decrease in the number of nuclei per syncytia (Figure 4).

Thus, the potency of a peptide or protein with Leu at position 679 is greatest and that with Ile is least active, with Ala and Val being intermediate. There is no simple rationale that can explain this order. Leu and Ile are the most hydrophobic, both having four carbon atoms in the side chain, yet they represent the two extremes of activity. The least hydrophobic amino acid is Ala, and this residue makes a more fusogenic protein than Ile. The two β-branched residues used are Ile and Val, yet they give proteins and peptides that are not very different from that with Ala, the least substituted residue used. Interestingly, the reduced fusogenicity of the mutant forms of gp41 correlates with the lowered interaction of the corresponding peptides with cholesterol in simple lipid mixtures.

REFERENCES

1. Salzwedel, K., West, J. T., and Hunter, E. (1999) A conserved tryptophan-rich motif in the membrane-proximal region of the human immunodeficiency virus type 1 gp41 ectodomain is important for Env-mediated fusion and virus infectivity, *J. Virol. 73*, 2469−2480.
2. Bellamy-McIntyre, A. K., Lay, C. S., Baar, S., Maerz, A. L., Talbo, G. H., Drummer, H. E., and Poumbourios, P. (2007) Functional links between the fusion peptide-proximal polar segment and membrane-proximal region of human immunodeficiency virus gp41 in distinct phases of membrane fusion, *J. Biol. Chem. 282*, 23104−23116.
3. Vincent, N., Genin, C., and Malvoisin, E. (2002) Identification of a conserved domain of the HIV-1 transmembrane protein gp41 which interacts with cholesteryl groups, *Biochim. Biophys. Acta 1567*, 157−164.
4. Epand, R. M., Sayer, B. G., and Epand, R. F. (2003) Peptide-induced formation of cholesterol-rich domains, *Biochemistry. 42*, 14677−14689.

5. Li, H., and Papadopoulos, V. (1998) Peripheral-type benzodiazepine receptor function in cholesterol transport. Identification of a putative cholesterol recognition/interaction amino acid sequence and consensus pattern, *Endocrinology 139*, 4991−4997.
6. Palmer, M. (2004) Cholesterol and the activity of bacterial toxins, *FEMS Microbiol. Lett. 238*, 281−289.
7. Epand, R. F., Thomas, A., Brasseur, R., Vishwanathan, S. A., Hunter, E., and Epand, R. M. (2006) Juxtamembrane protein segments that contribute to recruitment of cholesterol into domains, *Biochemistry 45*, 6105−6114.
8. Privalov, G., Kavina, V., Freire, E., and Privalov, P. L. (1995) Precise scanning calorimeter for studying thermal properties of biological macromolecules in dilute solution, *Anal. Biochem. 232*, 79−85.
9. Thomas, A., Deshayes, S., Decaffmeyer, M., Van Eyck, M. H., Charloteaux, B., and Brasseur, R. (2006) Prediction of peptide structure: How far are we? *Proteins 65*, 889−897.
10. Lins, L., Brasseur, R., De Pauw, M., Van Biervliet, J. P., Ruysschaert, J. M., Rosseneu, M., and Vanloo, B. (1995) Helix−helix interactions in reconstituted high-density lipoproteins, *Biochim. Biophys. Acta 1258*, 10−18.
11. Leach, A. R. (1996) van der Waals Interactions, in *Molecular Modelling: Principles and Applications* (Leach, A. R., Ed.) pp 171−177, Longman Ltd., Harlow, England.
12. Moult, J., and James, M. N. (1986) An algorithm for determining the conformation of polypeptide segments in proteins by systematic search, *Proteins 1*, 146−163.
13. Thomas, A., Milon, A., and Brasseur, R. (2004) Partial atomic charges of amino acids in proteins, *Proteins 56*, 102−109.
14. Brasseur, R. (1995) Simulating the folding of small proteins by use of the local minimum energy and the free solvation energy yields native-like structures, *J. Mol. Graphics 13*, 312−322.
15. Lins, L., Thomas, A., and Brasseur, R. (2003) Analysis of accessible surface of residues in proteins, *Protein Sci. 12*, 1406−1417.
16. Ducarme, P., Rahman, M., and Brasseur, R. (1998) IMPALA: A simple restraint field to simulate the biological membrane in molecular structure studies, *Proteins. 30*, 357−371.
17. Wei, X., Decker, J. M., Liu, H., Zhang, Z., Arani, R. B., Kilby, J. M., Saag, M. S., Wu, X., Shaw, G. M., and Kappes, J. C. (2002) Emergence of resistant human immunodeficiency virus type 1 in patients receiving fusion inhibitor (T-20) monotherapy, *Antimicrob. Agents. Chemother. 46*, 1896−1905.
18. Kimpton, J., and Emerman, M. (1992) Detection of replication-competent and pseudotyped human immunodeficiency virus with a sensitive cell line on the basis of activation of an integrated beta-galactosidase gene, *J. Virol. 66*, 2232−2239.
19. Epand, R. M. (2007) Detecting the presence of membrane domains using DSC, *Biophys. Chem. 126*, 197−200.
20. Epand, R. M., Bach, D., Borochov, N., and Wachtel, E. (2000) Cholesterol crystalline polymorphism and the solubility of cholesterol in phosphatidylserine, *Biophys. J. 78*, 866−873.
21. Loomis, C. R., Shipley, G. G., and Small, D. M. (1979) The phase behavior of hydrated cholesterol, *J. Lipid Res. 20*, 525−535.
22. Epand, R. M. (2004) Do proteins facilitate the formation of cholesterol-rich domains? *Biochim. Biophys. Acta 1666*, 227−238.
23. Brasseur, R. (1991) Differentiation of lipid-associating helices by use of three-dimensional molecular hydrophobicity potential calculations, *J. Biol. Chem. 266*, 16120−16127.
24. Zwick, M. B., Jensen, R., Church, S., Wang, M., Stiegler, G., Kunert, R., Katinger, H., and Burton, D. R. (2005) Anti-human immunodeficiency virus type 1 (HIV-1) antibodies 2F5 and 4E10 require surprisingly few crucial residues in the membrane-proximal external region of glycoprotein gp41 to neutralize HIV-1, *J. Virol. 79*, 1252−1261.
25. Lin, X., Derdeyn, C. A., Blumenthal, R., West, J., and Hunter, E. (2003) Progressive truncations C terminal to the membrane-spanning domain of simian immunodeficiency virus Env reduce fusogenicity and increase concentration dependence of Env for fusion, *J. Virol. 77*, 7067−7077.
26. Thomas, A., Milon, A., and Brasseur, R. (2004) Partial atomic charges of amino acids in proteins, *Proteins 56*, 102−109.

BI7018892